Journal of Power Sources 193 (2009) 285–291

Contents lists available at ScienceDirect

Journal of Power Sources

journal homepage: www.elsevier.com/locate/jpowsour

Hydrogen release properties of lithium alanate for application to fuel cell propulsion systems

P. Corbo*, F. Migliardini, O. Veneri

Istituto Motori – National Research Council (CNR), Via Marconi, 8 – 80125 Naples, Italy

ARTICLE INFO

Article history:
Received 9 October 2008
Received in revised form 4 December 2008
Accepted 22 December 2008
Available online 15 January 2009

Keywords:
Fuel cell power train
Electric vehicles
Lithium alanate
Hydrogen storage

ABSTRACT

In this paper the results of an experimental study on $LiAlH_4$ (lithium alanate) as hydrogen source for fuel cell propulsion systems are reported. The compound examined in this work was selected as reference material for light metal hydrides, because of its high hydrogen content (10.5 wt.%) and interesting desorption kinetic properties at moderate temperatures. Thermal dynamic and kinetic of hydrogen release from this hydride were investigated using a fixed bed reactor to evaluate the effect of heating procedure, carrier gas flow rate and sample form. The aim of this study was to characterize the lithium alanate decomposition through the reaction steps leading to the formation of Li_3AlH_6 and LiH. A hydrogen tank was designed and realized to contain pellets of lithium alanate as feeding for a fuel cell propulsion system based on a 2-kW Polymeric Electrolyte Fuel Cell (PEFC) stack. The fuel cell system was integrated into the power train comprising DC–DC converter, energy storage systems and electric drive for moped applications (3 kW). The experiments on the power train were conducted on a test bench able to simulate the vehicle behaviour and road characteristics on specific driving cycles. In particular the efficiencies of individual components and overall power train were analyzed evidencing the energy requirements of the hydrogen storage material.

1. Introduction

Environmental and oil dependence issues justify the strong research interest towards novel propulsion systems characterized by low pollutant emissions and high energy efficiency. In particular, the use of a hydrogen fuel cell system as an energy generator for electric power trains could improve the performance of electric vehicles by incrementing the driving range without compromising their crucial characteristic of local zero emissions [1–3]. The possibility to adopt such innovative electric vehicles would stimulate in short-medium term the creation of the infrastructures for the distributed hydrogen production in micro- and mini-plants, with consequent benefits on the diffusion of a public and private transportation system with zero environmental impact.

On board hydrogen storage is the main problem to be deal with for the successful implementation of fuel cell technology in the transportation sector. In particular, an acceptable on board storage device must be safe, lightweight and compact. The on board storage methods currently under consideration for prototyping include the usage of (i) high pressure gas, (ii) low temperature liquid, (iii) solid-state hydride hydrogen tanks. Though gas compression appears to be the simplest way to store hydrogen, the low storage mass and volume densities, together with high energetic costs for the compression step, high costs of 35–70 MPa tanks, and related safety problems, might hinder the commercial acceptation of this method. On the other hand, the relatively large amount of energy required by liquefaction, the necessity for on board cryogenic systems to keep temperatures between 20 and 30 K, and the continuous evaporation of liquid from the tank, limit this storage system for practical utilizations. An alternative method with interesting future perspectives consists in hydrogen adsorption on solid materials, in particular hydride based on light elements, such as alkali and alkaline-earth metals. These materials are characterized by acceptable storage capability but poor kinetic properties at moderate temperature [4]. Recently, the possibility to use metal-doped aluminium hydrides as potential hydrogen storage material has been reported [5–7], but reversibility and kinetic of the hydrogen adsorption/desorption cycle are critical issues to be carefully considered. Among lightweight metal hydrides the lithium alanate ($LiAlH_4$) is widely studied for its characteristics of significant hydrogen content (10.5 wt.% based on compound stoichiometry), favourable release kinetics at relatively low temperatures, and possibility to transform it in a different phase (Li_3AlH_6) [8–10], which still contains a theoretical hydrogen amount useful for automotive applications and whose decomposition was demonstrated to be reversible [11].

In previous papers we characterized fuel cell propulsion systems of different size by using high pressure hydrogen cylinders as fuel tanks [12–15]. These works demonstrated the great potentialities

* Corresponding author.
E-mail address: p.corbo@im.cnr.it (P. Corbo).

0378-7753/$ – see front matter © 2008 Elsevier B.V. All rights reserved.
doi:10.1016/j.jpowsour.2008.12.142

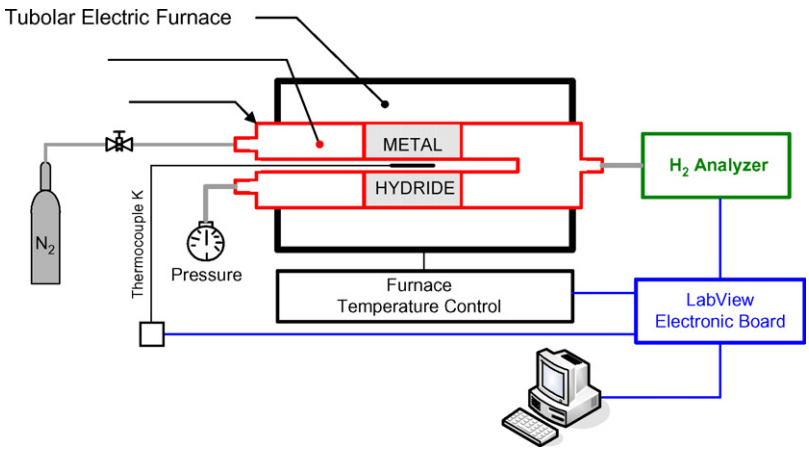

Fig. 1. Scheme of the laboratory reactor used for characterization of lithium alanate.

of fuel cell power trains in terms of energy efficiency with respect to conventional internal combustion engines, and evidenced the main issues to be faced regarding the energy management inside the propulsion system. The present paper deals with the problems related to hydrogen adsorption technology for fuel cell power train development. The lithium alanate ($LiAlH_4$) was selected as reference compound among light metal hydrides, and was firstly investigated analyzing the effect of thermal management (heating procedure and carrier gas flow rate) on control of hydrogen release, which is necessary in view of a practical application of the hydride to fuel cell power trains.

Moreover a specific device for utilization of adsorbent materials as hydrogen source in fuel cell propulsion systems for road applications was designed and realized, in order to obtain indications regarding the hybridization strategies to be adopted as function of hydrogen release properties of the storage material, and a first evaluation of its impact on the overall efficiency of a fuel cell power train running in real conditions (European driving cycle by dynamic test bench). These evaluations were performed on a fuel cell power train of 3 kW, suitable for moped applications [12].

2. Experimental

The pellet-shaped lithium alanate used in this work was purchased by Sigma–Aldrich (about 0.5 g each). The samples were characterized in laboratory tests evaluating the hydrogen release properties as function of temperature. These experiments were carried out by using a fixed bed reactor made of pyrex glass and heated by a tubular electric furnace equipped with a temperature controller (Fig. 1). The reaction temperature was measured by using a K type thermocouple inserted axially into the reactor, while a nitrogen flow was adopted as carrier during hydrogen release tests. The lithium alanate samples were loaded in the reactor in three forms, as pellets as delivered by the manufacturer, as fragment of an original pellet and as powder (<100 μm) obtained by manual pounding of the original pellets in an agate mortar. The gas pressure inside the reactor was measured by a manometer, and was maintained below 0.5 bar. The hydrogen concentration at the reactor outlet was measured by a Caldos 17 ABB on line analyzer equipped with TCD detector, while a mass flow controller was adopted for the nitrogen flow rate. Reaction temperature and hydrogen concentration at the reactor outlet were continuously acquired by a National Instrument acquisition board managed by LabView software.

The scheme of the storage tank for laboratory tests on fuel cell propulsion systems is shown in Fig. 2. The tank was designed and realized for utilization of different solid materials as hydrogen source for fuel cell systems based on PEFC stacks. It was made in stainless steel and equipped with temperature and pressure sensors. An electric resistance was placed coaxially inside the tank in order to supply the energy necessary to the hydrogen release from the material under test. This resistance was controlled by an external electric supplier. The volume was about 7 l, sufficient to feed a small size fuel cell propulsion system for scooter application (about 3 kW). For the experiments effected with this device $LiAlH_4$ pellets were loaded inside the tank, pressurizing the empty volume by hydrogen (99.999%) at 1 relative bar.

The overall scheme of the fuel cell system with the indication of the individual sub-systems is shown in Fig. 3. In this system the stack was equipped with other auxiliaries for its correct operation, i.e. air, water and heat management devices [13], while the device shown in Fig. 2 is utilized as hydrogen source for the stack. The details of the 3 kW fuel cell power train used in this work are reported in [12].

3. Results and discussion

The results of desorption tests conducted on lithium alanate are shown in Figs. 4–8, where the hydrogen flow rate measured at the reactor outlet is reported versus time (test length). A heating rate of 2 K min^{-1} and a nitrogen flow rate of 0.6 Nl min^{-1} were used during the tests of Figs. 4 and 5, where also the reaction temperature versus time is shown. The experiment of Fig. 4 was conducted on lithium alanate in the same form as provided by the manufacturer (pellet, 12 mm diameter, 4 mm height, 0.55 g weight). The profile of hydrogen release rate in Fig. 4 shows two evident peaks, although they are not completely separated, with maximum at 448 and 488 K, respectively, characterized by different slopes at light off points (45 and 65 s). The reaction temperature curve shows a slight increase with respect to the imposed heating rate, in correspondence of the first hydrogen flow rate peak. DTA analysis performed on Sigma–Aldrich lithium alanate in powder form [8] evidenced that the endothermic fusion of the hydride $LiAlH_4$ is accompanied by exothermic effects in the temperature range 423–473 K. On this base we can associate the first peak observed in Fig. 4 with the exothermic hydrogen release occurring during the decomposition of $LiAlH_4$, which produces Li_3AlH_6 according to the following reaction:

$$3LiAlH_4 = Li_3AlH_6 + 2Al + 3H_2 \quad (1)$$

The evaluation of the area underneath the first peak of Fig. 4 permitted to determine the hydrogen release percentage for the first reaction, which resulted 4.7 wt.% as H_2, in good agreement with the theoretical value (5.3 wt.%) obtainable from Eq. (1).

Regarding the second peak observed in Fig. 4, it can be attributed to the endothermic decomposition of Li_3AlH_6 [8] according to the

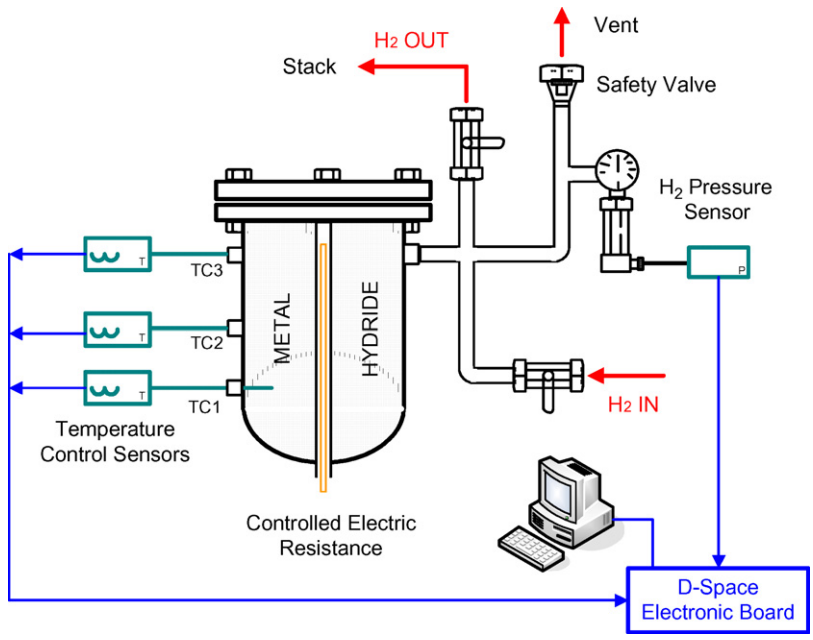

Fig. 2. Scheme of the laboratory device for utilization of light metal hydrides as fuel source in a fuel cell propulsion system.

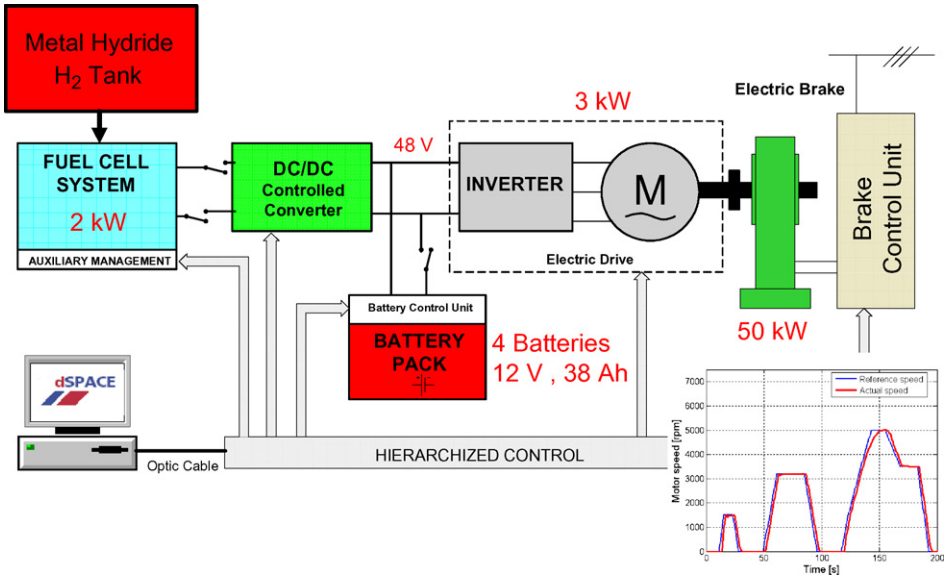

Fig. 3. Scheme of the fuel cell propulsion system fed with the laboratory metal hydride hydrogen tank and coupled to a dynamic test bench.

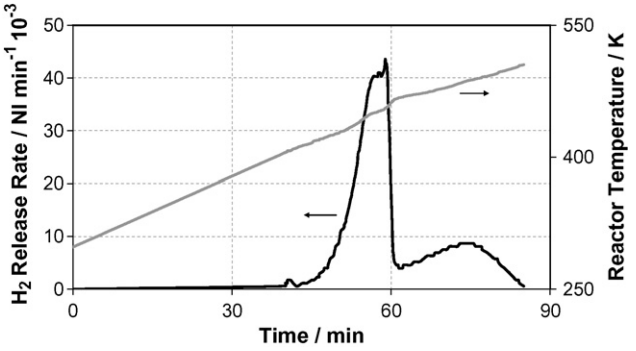

Fig. 4. Hydrogen release test on lithium alanate in pellet form (0.55 g). Heating rate: 2 K min^{-1}. Nitrogen flow rate: 0.6 Nl min^{-1}.

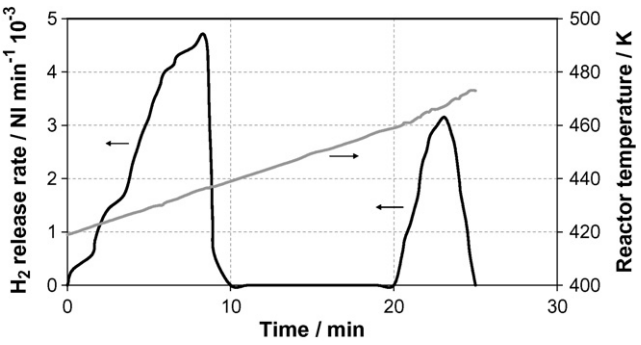

Fig. 5. Hydrogen release test on lithium alanate in pellet form (0.058 g, a fragment of a fresh pellet). Heating rate: 2 K min^{-1}. Nitrogen flow rate: 0.6 Nl min^{-1}.

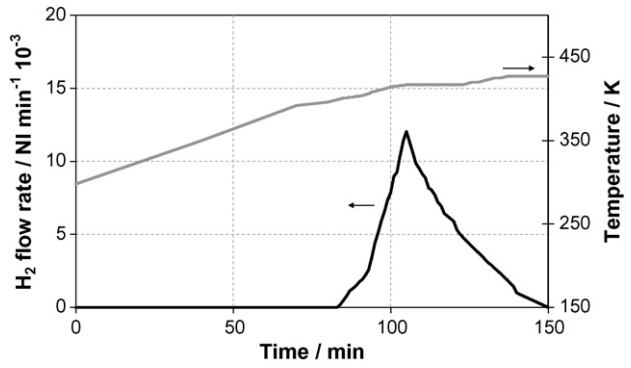

Fig. 6. Hydrogen release test on lithium alanate in pellet form (0.55 g). Heating rate: 1 K min^{-1} up to 400 K, average 0.25 K min^{-1} up to 425 K, cooling to room temperature. Nitrogen flow rate: 1 Nl min^{-1}.

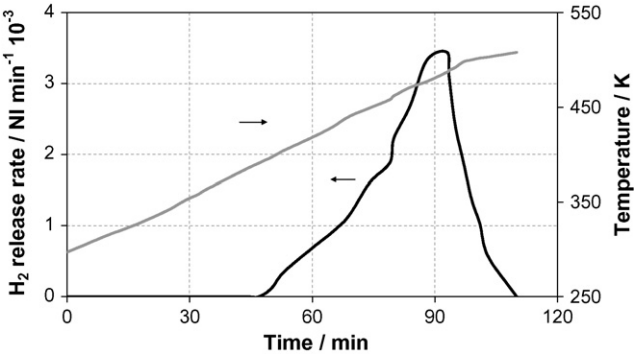

Fig. 7. Hydrogen release test on the same sample of Fig. 6 after reduction to powder form (<100 μm). Heating rate: 2 K min^{-1}. Nitrogen flow rate: 1 Nl min^{-1}.

following reaction:

$$Li_3AlH_6 = 3LiH + Al + 3/2H_2 \quad (2)$$

The integration of the second peak in Fig. 4 gives a hydrogen loss of 2 wt.%, compared to the theoretical value obtainable from reaction (2), which is 2.6 wt.% with respect to the starting material ($LiAlH_4$).

A further decomposition of LiH would be possible, according to the following equation:

$$3LiH + 3Al = 3LiAl + 3/2H_2 \quad (3)$$

However this reaction, which could provide an additional hydrogen contribution of 2.6 wt.%, was not considered, as it occurs at temperatures too high for an automotive application (about 673 K) [9].

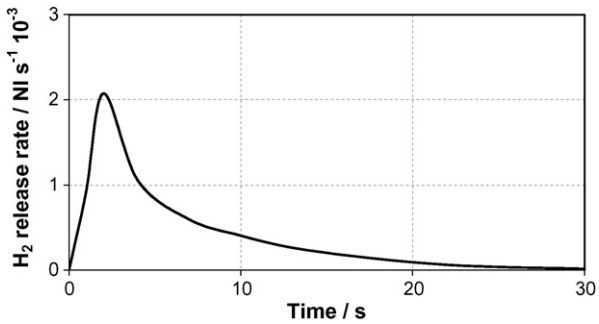

Fig. 8. Hydrogen release test on lithium alanate in powder form (<100 μm, 0.058 g). Heating rate: 2 K min^{-1}, nitrogen flow rate: 0.6 Nl min^{-1}. The hydrogen release started at 416 K.

The uncompleted separation of the two peaks in Fig. 4, together with the minor quantity of hydrogen released with respect to the theoretical values of reactions ((1) and (2)), suggest the following observations: (i) a fraction of hydrogen associated with the decomposition of $LiAlH_4$ can be released also for simple handling of the sample at room temperature during reactor loading, favoured by contact with air, (ii) the Li_3AlH_6 decomposition starts at about the same temperature as the first reaction, being affected by the exothermic effects associated with the $LiAlH_4$ decomposition. This behaviour appears confirmed by the results shown in Fig. 5, where the hydrogen flow rate measured at the reactor outlet is reported versus time for an experiment carried out on a fragment of a fresh pellet (0.058 g). In this figure the two peaks corresponding to reactions (1) and (2), with maximum at 433 and 473 K, are completely separated, and the hydrogen loss calculated by the evaluation of the areas underneath the peaks resulted 3.5 and 1.4 wt.%, respectively.

The best separation between the two peaks in Fig. 5 can be attributed to the small size of the sample (about ten times lighter than the pellet used for the experiment of Fig. 4), which permitted a better heat removal from the sample during the first exothermic decomposition. On this hypothesis, the second decomposition started at the same temperature as the first one (similarly to the experiment of Fig. 4), but rapidly stopped being less affected by the thermal effects deriving from reaction (1). When furnace temperature increased, the hydrogen release associated with reaction (2) appeared as a neat second peak. The hydrogen release measured for the first peak (3.5 wt.%) confirms the scarce stability of $LiAlH_4$ already at room temperature mentioned before, which appears favoured also by the pellet fragmentation effected in the presence of air. The hydrogen released during the second decomposition resulted about half the theoretical value (1.4 with respect to 2.6 wt.%), suggesting that part of hydrogen released by reaction (2) was already present under the first peak.

The effect of thermal management on the desorption kinetic of lithium alanate was then investigated in order to obtain a neat separation of reaction steps (1) and (2), with the consequent quantitative transformation of $LiAlH_4$ to Li_3AlH_6. Whole pellets of $LiAlH_4$ was tested adopting the following procedure: the oven was heated from room temperature up to about 400 K varying the heating rate (1 and 2 K min^{-1}), then a lower and not constant heating rate (average of 0.25 K min^{-1}) was adopted up to 425 K for all tests, followed by cooling to room temperature. These two heating procedures were utilized at three different nitrogen flow rates (0.6, 1 and 2 Nl min^{-1}), and permitted to obtain a first hydrogen release, whose weight percentage with respect to the initial pellet mass is reported in Table 1 for all tests. The same pellets were then reduced in powder form (<100 μm) and heated again from room temperature to 530 K in nitrogen flow (1 l min^{-1}) at about 2 K min^{-1}, obtaining a second hydrogen release (Table 1). The results indicated that the optimal thermal management can be realized by the simultaneous effect of both speed of temperature change and carrier gas flow rate. In fact, the theoretical hydrogen release values corresponding to Eqs. (1) and (2) could be obtained only with the lower rate in the first phase of heating procedure (1 K min^{-1}) and with carrier gas flow rate value of 1 Nl min^{-1}, while an evident but not complete separation of the two release phenomena was observed with 2 K min^{-1} and 0.6 Nl min^{-1} of carrier gas. Considering that the carrier gas can act both as heat carrier and remover, the data of Table 1 suggest that the effect of heat carrier is prevailing at higher heating rate (2 K min^{-1}), while at 1 K min^{-1} a compromise between the two effects could be reached.

The results of experiments conducted with the procedure which permitted the best separation of reaction steps (1) and (2) are shown in Figs. 6 and 7 in terms of hydrogen flow rate measured at the reactor outlet versus test length. Fig. 6 shows that the first hydrogen release was obtained, with a maximum at 410 K, and an

Table 1
Hydrogen release values for two heating procedures and three carrier gas flow rates.

N_2 flow rate (Nl min^{-1})	1 K min^{-1} [a] (H_2 wt.%)		2 K min^{-1} [a] (H_2 wt.%)	
	1st H_2 release	2nd H_2 release	1st H_2 release	2nd H_2 release
0.6	7.3	0.5	4.9	2.2
1	5.4	2.5	5.9	1.5
2	7.0	0.8	8.1	0.0

[a] From room temperature up to 400 K, followed by the heating procedure described in the text.

area corresponding to the percentage of hydrogen loss (5.4%) practically equal to that imposed by the stoichiometry of Eq. (1). The second hydrogen release profile is shown in Fig. 7, where a maximum at 480 K is observed, corresponding to 2.5% of hydrogen loss, as required by Eq. (2).

The lower desorption kinetic of Li_3AlH_6, already observed in Fig. 4, is confirmed by comparing the slopes at the light off points in Figs. 6 and 7, in spite of the powder form used for the Li_3AlH_6 sample. On the other hand, some literature data evidence that the hydrogen release intrinsic kinetic of Eq. (2) is significantly lower with respect to Eq. (1), for which a strong effect of grain size was observed in isothermal desorption tests [16].

The desorption test reported in Fig. 8 seems confirm this hypothesis. In this figure the hydrogen release rate is shown as function of time for an experiment carried out on a sample of $LiAlH_4$ in powder form (<100 μm). Fig. 8 shows that the whole hydrogen release was completed after about 25 s, while it was impossible to distinguish the two peaks corresponding to reactions (1) and (2), but only a unique large and tailed peak of hydrogen release rate was detected. A heating rate of 2 K min^{-1} was adopted in this test, the desorption started at 416 K and finished before a different temperature could be revealed into the reactor. This result evidences that for the $LiAlH_4$ sample in powder form, with higher specific surface with respect to pellet samples previously considered, the hydrogen release due to the first decomposition was extremely fast, in such a way to strongly affect also the velocity of the second decomposition, determining the partial overlapping of the two peaks.

The calculation of the hydrogen released by integration of the area under the curve in Fig. 8 provided a value of 2.6 wt.%, which could be mainly attributed to the decomposition of the more stable hydride, Li_3AlH_6, according to Eq. (2). The sample of $LiAlH_4$ was prepared in powder form in the presence of air, as for the tests of Figs. 4 and 5, then the high hydrogen content corresponding to Eq. (1) was partially lost already at room temperature due to the high reactivity of $LiAlH_4$.

In Figs. 9 and 10 the results of an experiment carried out on the hydrogen storage tank connected to the 3 kW fuel cell power train are reported. The test bench was controlled in order to execute an European R40 cycle (about 200 s), while during this test the valve at the tank outlet was maintained open, and the DC–DC converter was controlled in order to draw a constant power from the stack (hard hybrid power train configuration [15]). The tank was loaded with 25 $LiAlH_4$ pellets (corresponding to about 13 g) and the hydrogen pressure over the adsorbent material was imposed at about 1 relative bar at room temperature. In Fig. 9 the temperature and pressure profiles during the tank heating are shown, in particular the temperature increase rate was progressively reduced from 4 to 0.5 K min^{-1} at 500 and 5000 s, respectively. The pressure profile showed the expectable increase associated to the temperature variation, while a very fast rise (in about 10 s) up to 3.6 bar was observed at 5500 s (420 K), due to the rapid hydrogen release corresponding to the total hydrogen loss of Eqs. (1) and (2). After some minutes to stabilize the pressure, the electric contact between stack and DC–DC converter was closed, permitting the hydrogen to fed the fuel cells and stack power to be drawn towards the electric drive and/or batteries. The decrease of hydrogen pressure observed between 5740 and 5970 s (Fig. 9) corresponded to the execution of a whole R40 driving cycle with the stack power fixed at about 300 W (Fig. 10). This value corresponded to the cycle average power, and then determined a battery state of charge at the end of the cycle equal to that initial. The final pressure value inside the tank, approximately equal to that initial, confirmed that the whole quantity of hydrogen released was consumed during the R40 cycle with the selected hybrid power train configuration.

Fig. 9 shows that only one pressure rise was observed when the temperature reached 420 K, in spite of the very slow heating procedure (about 0.6 K min^{-1} at the end of the test). It has to be considered that the experiment was conducted without gas flow through the device but in hydrogen atmosphere, then without the

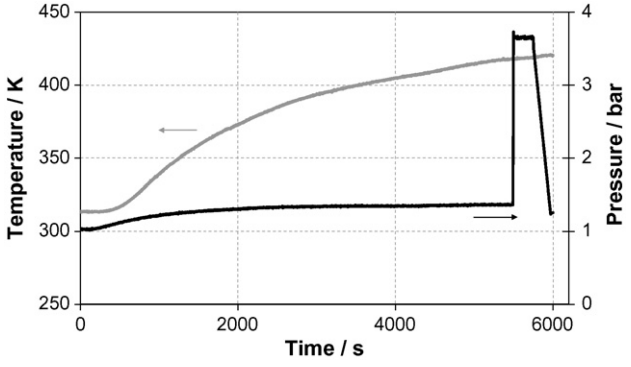

Fig. 9. Hydrogen release test on 13 g of lithium alanate in pellet form loaded in the laboratory storage tank coupled to the fuel cell power train. Heating rate decreasing from 4 to 0.5 K min^{-1}. Initial hydrogen pressure: 1 bar.

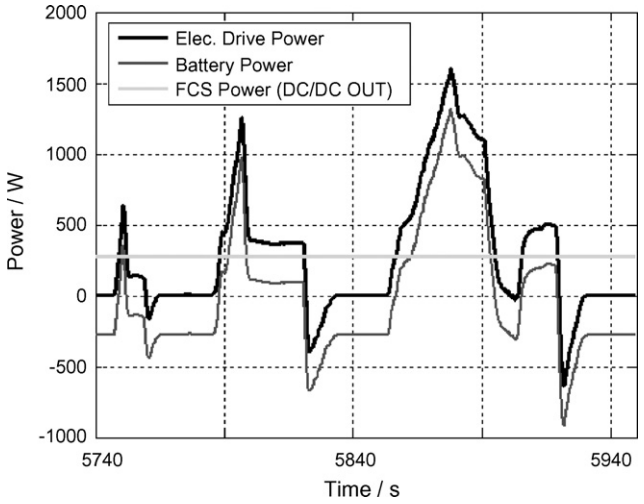

Fig. 10. Acquisition of powers supplied from the individual components of the 3 kW fuel cell power train fed with the hydrogen released from lithium alanate in the laboratory tank. Hard hybrid configuration, stack power = cycle average power (300 W).

heat removal associated to the convective flow. This implies that the exothermic effects due to reaction (1) determined also the fast occurring of reaction (2), without permitting the separation of the two hydrogen releases. This behaviour suggests some considerations about the characteristics required by a hydrogen storage system based on solid adsorbents.

For the vehicle considered in this work (electric scooter with 3 kW electric drive) a hydrogen tank of about 7 l is suitable. If this tank has to be used to assure a driving range of about 8 h on R40 cycle, a quantity of about 1850 g of lithium alanate has to be loaded inside the tank, corresponding to 2 l of volume occupied by the solid. With a fast hydrogen release like that shown in Fig. 9, which does not permit a gradual fuel release as a function of the power requirement, a maximum final pressure value of about 500 bar would be reached (calculated for a free volume of 5 l and 420 K). If the same tank of 7 l was filled with 144 g of compressed hydrogen (corresponding to all the hydrogen released by lithium alanate according Eqs. (1) and (2)), the total pressure would be about 350 bar. The only possibility to make the technology of hydrogen storage on solid materials practically convenient is to increase also the fuel volumetric density of the tank. This can be accomplished by the effective management of the hydrogen release rate as a function of stack power demands. This would imply the possibility to maintain low the pressure inside the tank, and finally to reduce its volume at parity of energy content. The possibility to control the release kinetic of the storage material can affect the hybridization strategy to be adopted in a fuel cell power train, i.e. the ratio between the power supplied by stack to that delivered by batteries. In particular, if the hydrogen release kinetic cannot be managed in a wide range of power demands, only a hybrid configuration characterized by steady state stack operation and intervention of batteries to satisfy engine dynamic requirements could be adopted.

The efficiencies of the power train components (fuel cell system, DC–DC converter, electric drive) and of the overall propulsion system were calculated for the experiment of Fig. 10 with the equations reported in [12,15], in particular the fuel cell system efficiency (η_{FCS}) was calculated as the ratio between the net power at DC–DC converter input and the theoretical power associated to the fuel entering the stack, while the DC–DC converter (η_{DC}) and electrical drive (η_{ED}) efficiencies were calculated as ratio between outlet and inlet power of the devices. Then the total efficiency of the power train (η_{PT}) on the driving cycle was determined by the following equation, assuming battery efficiency of 100% and taking back the final SOC to the initial level:

$$\eta_{PT} = \eta_{FCS}\eta_{DC}\eta_{ED} \quad (4)$$

The efficiencies of fuel cell system, DC–DC converter and electric drive resulted 47, 85 and 75%, respectively, while the total power train efficiency reached the value of 30% (Eq. (4)). In order to estimate the impact of the hydrogen storage technology based on adsorbent materials on the overall power train efficiency, the theoretical minimum energy consumption associated to the heating of lithium alanate from room temperature to 420 K (light off temperature, Fig. 9) was calculated. The result implied a minimum efficiency decrease of 10% with respect to the value obtainable with compressed hydrogen as stack feed (from 30 to 27% for total power train efficiency). In this first estimation the energy consumption of the real adsorption device was not considered, as a laboratory tank was utilized in this work, which is able to characterize different solid materials but not optimized for an application on vehicles. Moreover, the possibility of energy recovery deriving from the integration of the fuel storage device with the warm streams of the fuel cell system was also neglected.

Regarding the specific properties of the material used in this paper, it should be noticed that the standard Gibbs free energy at 25 °C for the $LiAlH_4$ decomposition to produce Li_3AlH_6 (Eq. (1)) is $\Delta G^\circ = -27.7\ kJ\ mol^{-1}$, which means that only kinetic limitation could hinder that reaction at room temperature [8]. On the other hand a strong catalytic effect on the velocity of this reaction has been observed by ball-milling $LiAlH_4$ with different substances, such as $TiCl_4$, $TiCl_3$, $AlCl_3$, $FeCl_3$, Ti, Fe, Ni, V, carbon black [10,17–19]. This catalytic effect resulted in a decrease of decomposition temperature and reduction of the first step of hydrogen evolution. In some cases ($TiCl_3$ and $TiCl_4$) this reduction was practically complete [10,17]. The results reported in this paper show that the first peak corresponding to the decomposition of $LiAlH_4$ can be partially lost also just handling the sample in the presence of air, and that this decomposition is strongly favoured by increasing the specific surface of the sample.

On the other hand some studies performed on the reversibility of lithium alanate decomposition [11] have demonstrated that LiH, Al and H_2 can be composed into Li_3AlH_6 at the presence of $LaCl_3$ catalyst, according to the reverse of Eq. (2), in conditions not too far from practical applications (180 °C, 8 MPa, 2 h), while no evidence is available about the reversibility of Eq. (1).

The US Department of Energy (DoE) has established a series of targets which should be met by hydrogen storage tanks, if a hydrogen-fuelled vehicle must match the performance of hydrocarbon-fuelled cars. Among these targets the gravimetric hydrogen density is considered crucial and the relative target of 6 wt.% very tough to meet [20]. The indication we can draw from the above results is that $LiAlH_4$ is an unsuitable material to meet the DoE requirements, but the practical usage of Li_3AlH_6 decomposition has to be considered, in order to improve its reversibility and kinetic properties by suitable catalysts. On the other hand also other lightweight hydrides characterized by sufficiently high hydrogen content and good reversibility properties in practically acceptable conditions should be investigated. At this regard, it could appear attractive to consider the properties of the hydride $NaAlH_4$, which can provide 5.5 wt.% of hydrogen under reasonable conditions, by a decomposition reaction that can be made reversible thanks to the usage of a catalyst [5]. However, also for this compound the high reactivity in the presence of air and moisture, especially in the presence of a catalyst, should be carefully addressed for practical applications.

The future work will be focused on two main issues. The properties of different light metal hydrides, including Li_3AlH_6, will be more closely examined, evaluating the possible improvement of their characteristics by adding other elements able to modify the adsorption/desorption cycle kinetics. Moreover, the dynamic behaviour of the hydrogen storage unit will be explored in order to verify the design issues of this specific component.

4. Conclusions

The potentialities of hydrogen storage technology based on complex light metal hydrides for automotive application were discussed choosing as reference material $LiAlH_4$ and using it in laboratory device coupled to a 3 kW fuel cell power train.

The properties of lithium alanate as hydrogen source for PEFC stacks were firstly investigated in laboratory tests using a fixed bed reactor and nitrogen as carrier gas. The overall hydrogen release resulted about 8% in two successive steps (decomposition of $LiAlH_4$, followed by decomposition of Li_3AlH_6) characterized by different kinetics, in the temperature ranges of 400–420 and 450–470 K, respectively. The effect of the heating procedure and carrier gas flow rate on the possibility to separate the two phases of hydrogen release was studied, in particular lowering the heating rate ($1\ K\ min^{-1}$) and adopting the optimal nitrogen flow rate (about $1\ l\ min^{-1}$) a neat separation between the two phenomena was

obtained. The effect of the grain size was also investigated, evidencing that only the kinetic of the first release was affected by this parameter, being the $LiAlH_4$ decomposition characterized by very high intrinsic kinetic. The management of hydrogen release by Eq. (1) ($LiAlH_4$ decomposition) resulted hardly obtainable, while the hydrogen release by Eq. (2) (Li_3AlH_6 decomposition) was more easily controlled.

The tests effected on the storage device coupled to the fuel cell power train evidenced the crucial issue of the pressure control inside the tank, in particular due to the high reactivity of lithium alanate very high hydrogen pressures were obtained in few seconds, hardly allowing the control of release kinetic in spite of the accurate management of temperature during the heating. In this view the hexahydride phase (Li_3AlH_6), obtained from decomposition of lithium alanate, resulted more promising, due not only to the potentialities regarding the reversibility of dehydrogenation, but also to its lower kinetic of decomposition, which implies the possibility of a better control of the tank pressure as function of the power demands, with the advantage of using low volumes, and increasing the volumetric density of the device.

Acknowledgment

The authors gratefully acknowledge Mr Giovanni Cantilena of Istituto Motori for his cooperation in realization of the experimental apparatus and execution of tests.

References

[1] M. Granovskii, I. Dincer, M.A. Rosen, Int. J. Hydrogen Energy 31 (2006) 337.
[2] R. Helmolt, U. Eberle, J. Power Sources 165 (2007) 833.
[3] P. Corbo, F.E. Corcione, F. Migliardini, O. Veneri, J. Power Sources 145 (2005) 610–619.
[4] Z.X. Guo, C. Shang, K.F. Aguey-Zinsou, J. Eur. Ceram. Soc. 28 (2008) 1473–1476.
[5] B. Bogdanovic, R.A. Brand, A. Marjanovic, M. Schwikardi, J. Alloy Compd. 302 (2000) 36–58.
[6] C.M. Jensen, R. Zidan, N. Mariels, A.A. Hee, C. Hagen, Int. J. Hydrogen Energy 24 (1999) 461–465.
[7] L. Zaluski, A. Zaluska, J.O. Strom-Olsen, J. Alloy Compd. 290 (1999) 71–78.
[8] V.B. Balema, V.K. Pecharsky, K.W. Dennis, J. Alloy Compd. 313 (2000) 69–74.
[9] D.S. Easton, J.H. Schneibel, S.A. Speakman, J. Alloy Compd. 398 (2005) 245–248.
[10] M. Resan, M.D. Hampton, J.K. Lomness, D.K. Slattery, Int. J. Hydrogen Energy 30 (2005) 1417–1421.
[11] Z. Xueping, L. Ping, I.S. Humail, A. Fuqiang, W. Guoqing, Q. Xuanhui, Int. J. Hydrogen Energy 32 (2007) 4957–4960.
[12] P. Corbo, F.E. Corcione, F. Migliardini, O. Veneri, J. Power Sources 157 (2006) 799–808.
[13] P. Corbo, F. Migliardini, O. Veneri, Int. J. Hydrogen Energy 32 (2007) 4340–4349.
[14] P. Corbo, F. Migliardini, O. Veneri, Energy Manage. Convers. 48 (2007) 2365–2374.
[15] P. Corbo, F. Migliardini, O. Veneri, J. Power Sources 181 (2008) 363–370.
[16] A. Andreasen, T. Vegge, A.S. Pedersen, J. Solid State Chem. 178 (2005) 3672–3678.
[17] M. Resan, M.D. Hampton, J.K. Lomness, D.K. Slattery, Int. J. Hydrogen Energy 30 (2005) 1413–1416.
[18] D. Blanchard, H.W. Brinks, B.C. Hauback, P. Norby, Mater. Sci. Eng. B108 (2004) 54–59.
[19] V.B. Balema, J.W. Wiench, K.W. Dennis, M. Pruski, V.K. Pecharsky, J. Alloy Compd. 329 (2001) 108–114.
[20] D.K. Ross, Vacuum 80 (2006) 1084–1089.